Evaluating bioelectrochemically-assisted constructed wetland (METland®) for treating wastewater: analysis of materials, performance and electroactive communities

Amanda Prado de Nicolás [a,b] , Raúl Berenguer [c], Abraham Esteve-Núñez [a,b,d*]

[a] Department of Analytical Chemistry, Physical Chemistry and Chemical Engineering, University of Alcalá, Alcalá de Henares, Spain

[b] IMDEA Water Institute, Alcalá de Henares, Madrid, Spain

[c] Instituto Universitario de Materiales, Departamento Química Física, Universidad de Alicante, Alicante, Spain

[d] METfilter, Carrión de los Céspedes, Spain

*corresponding author: Abraham Esteve-Núñez (abraham.esteve@uah.es)

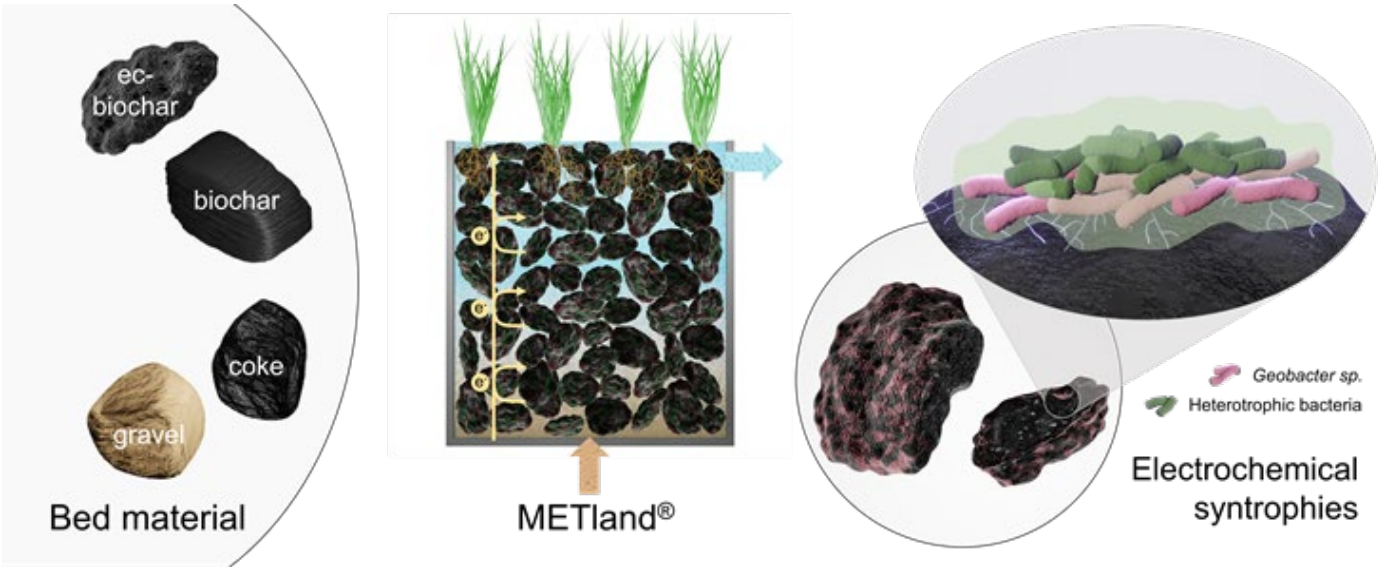

Abstract

METland® technology consists of a bioengineering strategy for treating wastewater by integrating microbial electrochemical concepts into constructed wetland systems to enhance pollutants removal. Under this configuration, we have constructed planted (*Iris sibirica)* and non-planted biofilters to assess the impact of different electrically conductive bed materials (electroconductive coke, electroconductive biochar, non-electroconductive biochar and gravel) by analyzing the (i) wastewater treatment efficiency (COD and nitrogen removal), (ii) bioelectrochemical response, and (iii) microbial community diversity. Biofilters with electrically conductive materials present the highest removal rates (175-180 gCOD/bed*m^3 day) and have a smaller footprint (0.4 m^2/pe). In contrast, the highest nitrogen removal rates were achieved with non-conductive biochar in presence of plants (80 % N-removal). This was supported by the presence of annamox bacteria like Planctomycetes. Furthermore, the electric potential profile along the bed depth in electrically conductive materials and the electrochemical analysis (cyclic voltammetry assays) demonstrated an effective electron flux from the bottom to the uppermost layers of the bed (geoconductor mechanism). In the electroconductive biochar, an effective conductivity-based model co-exists with a geobattery mechanism due to the presence of electroactive phenolic and carbonyl/quinone groups and/or microporosity. Microbial biodiversity analysis revealed that plants have an impact just at the upper layers of the biofilters, where roots and *Rhizobium* predominate. Bacteria from genus *Clostridium* were dominant in gravel inert material; in contrast, bacteria from genus *Geobacter* (12%) and *Trichococcus* (30%) outcompete the rest of communities for effective colonization of carbonaceous beds, suggesting their main role as part of the electrosyntrophies mechanism in METland®.

Key words: Microbial electrochemistry; constructed wetland; metland®; electroactive bacteria; wastewater treatment; electroconductive biochar.

1. Introduction

Nature-based solutions (NBSs) are technologies that rely on naturally occurring processes and simultaneously provide environmental, social and economic benefits. Indeed, they are a real solution to worldwide challenges like mitigating the deterioration of water resources caused by ineffective wastewater treatment [1]. Constructed wetlands (CWs) are a common example of NBS that mimic natural wetland to passively treat wastewater. Many CWs use substrates to support microorganisms and plants that can remove contamination from the water being treated [2,3]. This environmentally friendly technology has been widely implemented throughout the world due to its simple mode of operation, low cost, and high efficiency treating various types of wastewater [2,4]. However, compared to conventional biological treatments, CWs have a large footprint of land required and risk of clogging as main drawbacks [5]. Thus, there is a pressing need for exploring strategies to intensify pollutants removal in CWs.

To overcome this limitation, the integration of microbial electrochemical technologies (MET) with CWs represents a promising approach [6]. METs are based on the ability of electroactive bacteria (EAB) to exchange electrons with electrically conductive materials [7]. The EAB can oxidize pollutants present in wastewater that would be otherwise slowly degradable in conventional CWs because they transfer excess electrons to an electrically conductive bed materials so electron acceptor limitation is minimized [8]. The first attempt to incorporate METs into CWs aimed to harvest electrical energy from organic pollutants through the so-called constructed wetlands - microbial fuel cells (CW-MFCs) [9]. This strategy has shown success at lab scale for harvesting energy from complex wastewater [10–13] without clogging problems [14]; however, power generation higher than mW range seems difficult due to internal resistance between the electrodes, which increases linearly with the size and distance [15–17].

An alternative strategy to overcome the scaling limitations to merge MET and CW has recently generated a hybrid technology known as METland® [18]. This concept requires a complete replacement of the conventional bed material (gravel or sand) with an electrically conductive material, a never-ending source of terminal electron acceptor to support the microbial catabolism of pollutants [19,20]. Originally, METland® was designed to operate under flooded conditions and short-circuit mode based on a continuous bed of electrically conductive material [18], a similar mechanism to the one reported as “snorkel” electrodes [21]. The natural redox gradient between the bottom of the electroconductive bed and the naturally oxygenated surface greatly enhanced electroactive bacteria metabolism. The anodic oxidation of organic matter occurs in the anoxic bottom layers, these reactions are not limited since the electrically conductive material acts as an inexhaustible electron acceptor. The main cathodic process, like the reduction of oxygen, takes place at the upper bed layers [22]. The existence of such electron flow along the METland® bed was demonstrated by measuring the profile of electric potential along distances larger than 40 cm [6,22] and, interestingly, such electron flow can also be controlled by integrating artificial devices so-called e-sinks [22]. Full scale METlands® using large electroconductive carbonaceous-based biofilters, have been implemented in diverse geographic regions while achieving COD removal efficiencies of 90% [23]. Comparison METland® footprint versus conventional constructed wetlands is 7 times less (0.4m^2/pe versus 3m^2/pe respectively). Furthermore, they are proved to be environmentally sustainable after LCA analysis [24].

Conventional CWs include vegetation, which significantly affects the system, mainly, by up taking nutrients, excreting oxygen into the rhizosphere, providing a surface for bacterial attachment, supporting microbial community biodiversity, as well as preventing the substrate clogging [25,26]. However, the contribution of plants for nutrient removal in a METland® is not relevant compared to that of microorganism due to the high loading rate (ca. 15 gN/m^3

day) used to feed such bioelectrochemical systems [27]. In bioelectrochemical-assisted constructed wetlands like METland®, the electrically conductive carbonaceous material provides a competitive advantage for EABs [28] to efficiently interact with the bed material. These interactions promote the accepting and/or donating of electrons by creating electrochemical syntrophies [29] between bacteria which stimulate their metabolic activity allowing for increased removal rates.

Efficient extracellular electrons transfer (EET) is key for co-metabolic partnerships. There are two main pathways for EET. First, EET mediated by the conductive bed material itself (Conductive-particle-mediated Interspecies Electron Transfer/CIET) where the conductive particle acts as a vector for EET. The second is the direct exchange of electrons between microbes or Direct Interspecies Electron Transfer (DIET) [29]. The model electrogenic microorganism *Geobacter sulfurreducens* plays a key role in this electron transfer. It acts as a conduit between the heterotrophs that oxidize organic compounds and the electroconductive bed [30]. A recent study demonstrates that the physicochemical properties of the bed material, including the electrical conductivity, porosity, and surface chemistry, play a key role in the bacteria-material electron transfer [19]. Particularly, the electrically conductivity of the material may be crucial for effective electron transfer with bacteria, what has been referred to as the “geoconductor” e-transfer mechanism [31]. On the other hand, it has been proposed that certain surface oxygen groups on carbon materials, like electroactive phenol- and quinone-like functionalities, can reversibly exchange electrons with microorganisms in biogeochemical processes. These processes involving electrochemical reactions have been associated with the discontinuous e-transfer mechanism, so-called geobattery. Furthermore, the potential capability of carbons to storage these exchanged electrons, thus, acting as electron reservoirs in biogeochemical processes, has been designated as the “geocapacitor” behaviour [19]. A recent study suggest a

remarkable role of pyrogenic carbon for acting as alternative electron acceptor in soil while reducing release of methane [32].

This work aims to understand the complex functioning of a METland® and identify the key factors that determine the system's efficiency for wastewater treatment. We explored the impact of the physicochemical properties of different electrically conductive material (coke, electrically conductive biochar and non-electrically conductive biochar) on wastewater treatment efficiency. Finally, we explored how these properties, in combination with plants from *Iris sibirica genus,* affected the development of bacterial communities, specifically the role that *Geobacter* may play as a key electroactive bacterial genus in the performance of this solution.

2. Materials and Methods

2.1 Biofilters construction and bed materials

In this study, eight laboratory-scale up-flow biofilters were constructed (Fig. 1). Every biofilter consisted of a 2.2 L polyvinylchloride (PVC) cylinder (diameter: 90 mm, height: 35 cm) with an up-flow feed. One perforated pipe for sampling was placed inside every biofilter. In addition, at the bottom of each biofilter there was a sampler to take granules. Biofilters were filled with four different materials, in all cases the dead volume was approximately 50% of the total volume.

Each couple of biofilters was hosting the following materials: electroconductive coke (ecC), electroconductive biochar (ecB), non-electroconductive biochar (ncB) and gravel (G) as inert control, all supplied with same granulometry (1.5 – 3.0 cm) by METfilter SL. (Table S1).

Four biofilter made of all different materials were planted with *Iris sibirica* freshly harvested from the Botanical Garden from University of Alcalá, (Alcalá de Henares, Spain). In a first step, the plants were acclimatized to wastewater in a full-scale METland® (10 m^2) at IMDEA Water facilities. The wetland plants, with one rhizome density per unit, were rinsed three times with tap water before being transplanted to the biofilter of the current study. Their roots shown lengths of 7.5 ± 0.8 cm and plants had stems with an average length of 27.0 ± 2.4 cm.

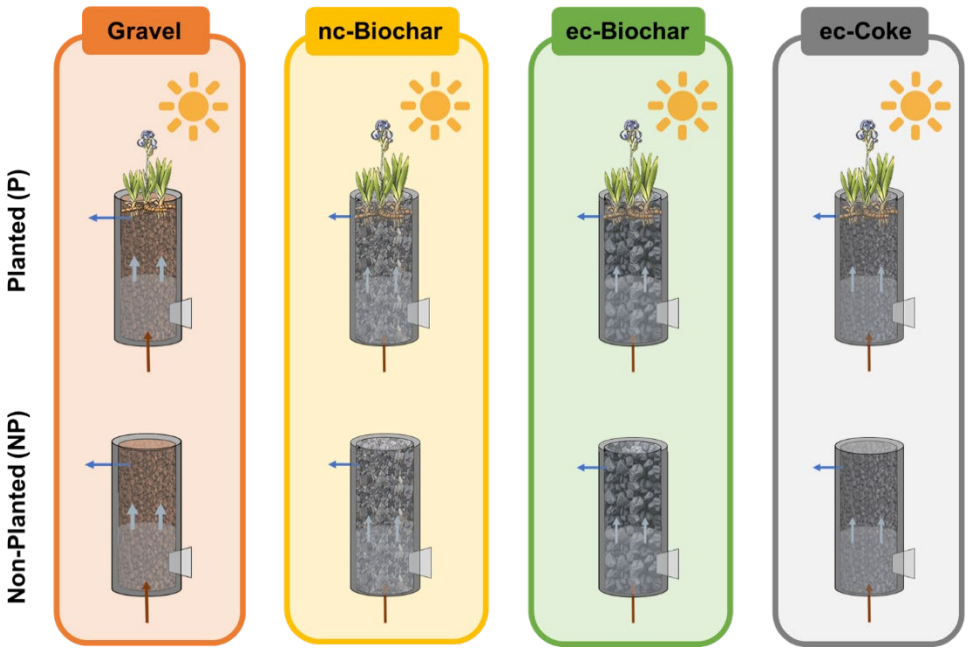

Fig. 1 Scheme of electrochemically-assisted biofilters made of four materials: (gravel, nc-biochar, ec-biochar and ec-coke) operating up-flow in absence or presence of plants.

2.2 Characterization of Bed materials

Electrical conductivity measurements were carried out by using a Lucas Lab resistivity equipment with four probes in-line [33]. For this characterization, ca. 200 mg of each sample in the form of granules were first crushed down to a fine powder, dried under vacuum for 24 h, and shaped into pellets of 0.013 m diameter by applying a pressure of $7.4 \cdot 10^8$ Pa. The porous texture of the as-provided samples granules (0.2-0.4 g) was characterized by N_2 adsorption-desorption at 196 ºC and by CO_2 adsorption at 0 ºC (in the case of microporous samples), using a Quadrasorb-Kr/MP (Quantrachrome Corporation) equipment. Samples were previously outgassed for 6 h at 150 ºC under vacuum. The specific surface area (S_{BET}) and the micropore volume ($V_{DR}(N_2)$) were calculated from the N_2 adsorption-desorption isotherms by using the BET and Dubinin-Radushkevich equations, respectively [34]. The mesopore volume (V_{mes}) was calculated as the difference between total pore volume ($V_{0.995}$, volume at relative pressure of 0.995) and micropore volume [34]. The narrow micropore

volume ($V_{DR}(CO_2)$) and the narrow micropore surface area ($A_{DR}(CO_2)$) were estimated for both types of biochar by applying the Dubinin-Radushkevich equation to the CO_2 adsorption isotherm [34]. The pore volume and dimensions of the as-provided samples granules (around 0.7 g) were further characterized by Hg intrusion-extrusion porosimetry, with a PoreMaster 60-GT porosimeter (Quantachrome Instruments) using a pressure range from 6.84 to 408330 kPa. The Washburn equation was utilized to relate the applied pressure with the pore diameter [35].

The amount and nature of surface oxygen groups present on the carbon materials were studied by temperature-programmed desorption (TPD) experiments in a simultaneous TGA/DSC 2 equipment (Mettler-Toledo) coupled to a mass spectrometer (ThermoStar GSD 301 T, Pfeiffer Vacuum). In these experiments, around 20 mg of the crushed (powdery) carbon samples were heated up to 1000 ºC at 20 ºC/min under a He flow rate of 100 mL/min. Upon heating, surface oxygen groups on carbon materials decompose producing CO and CO_2 at different temperatures as a function of their thermal stability [36]. The quantification of the evolved CO and CO_2 groups was done by using a calcium oxalate monohydrate calibration and considering the CO disproportionation.

2.3 Biofilter operation and water quality analysis

The eight biofilters (Fig. 1) were housed indoor, where the temperature was kept approximately constant at 27 ± 2 ºC, and enlightened for 12 hours/day with led lamp for indoor plants emitting from 380 nm to 800 nm. The systems were operated simultaneously in parallel to study the influence of several variables, highlighting the nature of the bed material and the presence of plants. In this study, the systems were fed with real urban wastewater pre-treated in an Imhoff tank (860 mg/L COD, 65 mg/L NH_4^+ and no NO_3^-) and operated in a continuous up-flow mode with a hydraulic retention time (HRT) of 2 days by the aid of a peristaltic pump (Watson-Marlow®).

The decontamination of wastewater in the different biofilters was followed by monitoring the chemical oxygen demand (COD) and concentration of N-containing species. For such a purpose, samples of the influent and effluent were taken from all systems every three days. The removal efficiencies in the outlets were calculated as percentage of the inlets, whereas the removal rates were obtained from the inlet-outlet differences as COD grams per cubic meter of bed material per day (g/m^3 • day). The analysis of these parameters indicated that a start-up period of 10 days was necessary to reach steady state operation conditions in all systems. During this transition period, various important processes showing different kinetics, including adsorption of molecules and biofilm formation, were stabilized to become negligible in the evaluated performance of the bioreactors.

The COD was analysed following a standard spectroscopic method [37], while the concentration of NH_4^+ and NO_3^- was monitored by ion chromatography using a Metrohm 930 Compact Ion Chromatograph Flex.

In addition, oxygen concentration in the biofilters was measured in-situ every 5 cm along the entire depth of the systems with a fiberopticoxygen meter (FireSting O2, Pyro-science). From these measurements, in-depth oxygen concentration profiles were constructed for the different biofilters.

2.4 Electrochemical measurements

2.4.1 Electric potentials profiles with depth

To measure the electric potential (EP) two reference electrodes shielded silver/silver chloride were used [22]. These reference electrodes are more insensitive to redox-active compounds than the liquid ones. One reference electrode was placed in the upper layer of the biofilter below the surface of the water. Both electrodes were connected to a digital voltmeter. The difference of the potential between both reference electrodes was measured

along depth every three centimeters in all the systems. These profiles were performed in each of the eight systems at time 0 (abiotic conditions) during the start-up period (10 days) and in the steady state (20 days), all of them with wastewater as electrolyte. The overlying water signal value was used as a reference potential to normalized all the profiles. This value was subtracted from all the values in the profile. The results are a normalized electric potential depth profile.

2.4.2 Cyclic voltammetry of single granules

The microbial electrochemical response was studied by cyclic voltammetry (CV) in a single chamber cell. Single granule CVs were performed in the upper and lower location of every biofilter. From each, three independent granules (considered as replicas) of ca. 1 cm^2 were selected from upper and lower environment of every biofilter. A butyl septum sealing the lower part of the system was used to access the lowermost bed. Furthermore, every granule was perforated and hooked by a non-conductive thread so they could be easily identified and selected during the course of the experiment (Fig. S1). Actually, granules were back to the biofilter after CV analysis. Such procedure allows bacterial biofilm to grow during the course of the assay.

The CV experiments were carried out in a conventional three-electrodes single chamber (Fig. S1). The scan rate was 10 mV/s and the potential range was between -0.6 V and 0.6 V (*vs*. Ag/AgCl). The reference electrode was a HANNA HI-5311 glass body Ag/AgCl (sat.) electrode with ceramic junction. The counter electrode was a 2x3 cm Ti/Pt mesh, attached to a copper wire protected by heat shrink tubing. The working electrode was each of the selected single granules. In order to avoid corrosion on the electrical connexion, between the granule and the wire, it was used a gold wire [38]. All the electrodes were immersed in anaerobic phosphate buffer 100mM deoxygenated with N_2 and acetate 10mM. Three CVs

cycles were performed to each sample at three different times: t0 (abiotic conditions), t10 days (start-up period) and t20 days (steady state).

2.5 Microbial communities and data analysis

2.5.1 16S Metagenomic Sequencing

To analyse the microbial diversity and composition of biofilms grown on different biofilter materials and bed locations, a sample of bed granules (ca. 15ml) was taken from top and bottom parts of each biofilter. The samples were stored at -20ºC before DNA extraction. The DNA extraction, PCR amplification, and high-throughput sequencing were performed by external service for genomic analysis (Institute of Biotechnology and Biomedicine, UAB, Barcelona).

The V3-V4 region of the 16Sr DNA bacterial gene was amplified by a polymerase chain reaction (PCR) using the 338F/806R primers. The protocols of this analysis were set according to Klindworth et al. [39]. A high-throughput sequencing analysis was conducted using Illumina- MiSeq from Servei de Genòmica i Bioinformàtica (Barcelona, Spain).

2.5.2 Scanning electron microscopy SEM

The morphology of biofilms grown on different materials was analyzed by scanning electron microscopy (SEM). For this analysis, granules of different materials were taken from the upper and lower sections of biofilters in each reactor (16 samples in total). The granule-associated biofilm was fixed in 5% (v/v) glutaraldehyde in 0.2 M sodium cacodylate pH 7.2 for 60 min. Granules were then washed twice with 0.2 M sodium cacodylate pH 7.2 for 10 min. The fixed granules were dehydrated in ethanol series (sequentially in 25, 50, 70, 90 and 100 % ethanol for 10 min each), acetone 100 % 10 min and anhydrous acetone for 12 h in a refrigerator. Next, the fixed granules were dried with a critical-point drier using liquid

CO_2 and finally coated with gold by sputtering at 100 V and 100 mA for 2 min (E1030, Hitachi, Spain). The coated granules were examined with a DSM 950 microscope (Zeiss) at 3.5 kV.

2.6 Statistical analysis

Removal efficiencies were calculated as a percentage of the total COD or nitrogen influent concentration. Removal rates were obtained from the inlet-outlet difference as grams per cubic meter of bed per day. The values include in the bar graphs correspond to the average value of the measurements taken at each operation period (start-up and steady state). The error bars in the bar graphs represent the standard error of the mean.

The alpha diversity index, including Shannon and Simpson diversity index, ACE and Chao1 estimation (Table S5) and the dendrogram (Fig. S14) and PCoA graphs (Fig. S11), were provided by the Servei de Genòmica i Bioinformàtica (Barcelona, Spain).

3. Results and discussion

Nature-based solutions, like constructed wetlands, are a sustainable technology for treating urban wastewater where bed material is a matter of current research. Actually, the use of electroconductive material for making the biofiltering bed led to large enhancement in microbial biodegradation of organic pollutants as shown by recent studies [20,40]. In this context, we aimed to explore the impact of the bed material and plants from genus *Iris sibirica* regarding: i) treatment efficiency (COD and nitrogen removal), ii) microbial diversity and iii) bioelectrochemical response.

3.1 Characterization of biofilter materials: physico-chemical properties

The textural, structural and chemical properties of the bed materials play a key role on the microbial activity and/or colonization, so the four materials: gravel, ec-coke, ec-biochar and nc-biochar were characterized. The features of the gravel and ec-coke were previously

reported [19]. Essentially, the siliceous material did no present electrical conductivity and a very smooth surface without micro- (diameter (d) < 2 nm), meso- (2 < d < 50 nm) or macro-pores (d > 50 nm). On the contrary, the ec-coke exhibited a high conductivity of ~10.4 S/cm (Fig. 2A) and a remarkable rough morphology (Fig. 2B) which accounts for a porosity of 37 % (Fig. 2C), as deduced from Hg intrusion curves (Fig. S2). Besides, this material stands out for its poor surface chemistry, with a low content of oxygen functionalities (Fig. 2E), and the lack of micropores (Fig. 2C) and mesopores (see TPD curves and N_2 adsorption-desorption isotherms in Fig. S3 and S4, respectively).

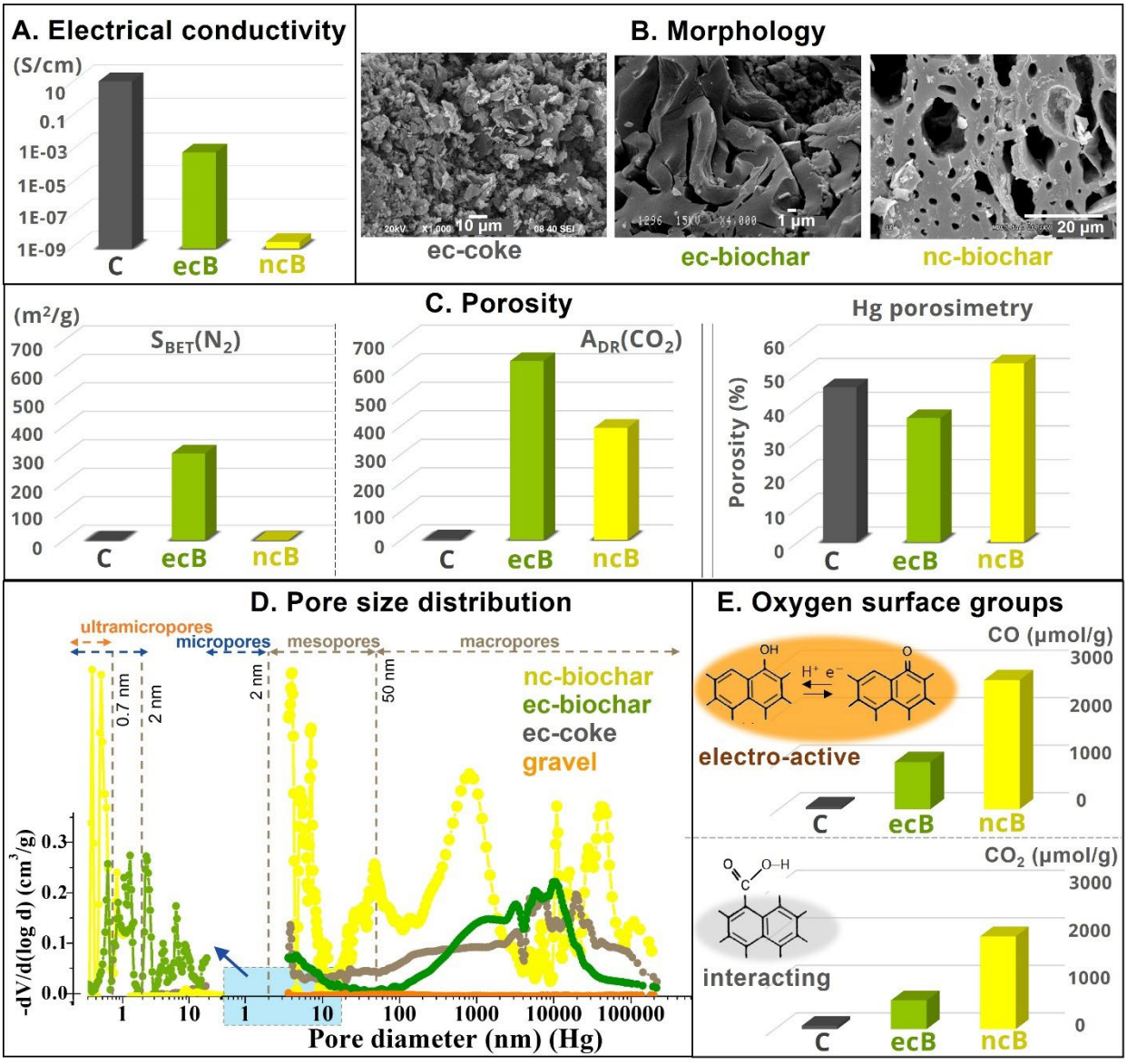

Fig. 2. Main physico-chemical properties of the carbonaceous biofilter materials, including the electrical conductivity (A); morphology (SEM images, B); porosity (BET and $A_{DR}(CO_2)$ specific surface areas and % porosity in C); pore size distribution (D); oyxgen surface groups (CO_2-like and CO-like evolving groups from TPD in E).

Regarding the two types of biochars, the main distinguishing feature was their electrical conductivity (Fig. 2A). The conductive one (ec-biochar) showed a conductivity of 0.6 mS/cm, which was 5 orders of magnitude larger than the one measured for non-conductive biochar ($2.6E10^{-6}$ mS/cm), but much lower (ca. 18000 times) compared to that of the ec-coke (~10.4 S/cm). These differences were attributed to their different graphitic microstructures (Fig. S5) that, in fact, may arise from their distinct precursors and preparation conditions.

On the other hand, both type of biochar displayed exclusive textural and chemical properties. First, the biochar samples exhibited more uniform pores than the others materials used as bed (Fig. 2B), typical of vascular and cellular systems of the vegetal precursors [19]. Particularly, the ec-biochar presented distorted slit-like pores (Fig. 2B), but quite a similar percentage of macroporosity (about 40 % in Fig. 2C) and pore size distribution (between 0.1 and 40 μm, in Fig. 2D) compared to the ec-coke. For the nc-biochar, well-defined cylindrical channels of variable size were observed (Fig. 2B). In this sense, the defined peaks in the pore size distribution of this material (Fig. 2D) reflected the uniformity of its pore structure, revealing also the existence of smaller pores of less than 100 nm. Accordingly, the % of porosity in the nc-biochar was considerably larger than that for the other tested carbon materials (ca. 54 % in Fig. 2C).

Second, both biochar exhibited a well-developed microporosity, and especially narrow microporosity (as deduced from $A_{CO2} > S_{BET}$), which was larger in the case of the ec-biochar (Fig. 2C). In this sense, it should be stressed that the micropores of the nc-biochar were so narrow that they were inaccessible to N_2 gas probe (see N_2 adsorption-desorption isotherm in Fig. S4). By contrast, the ec-biochar showed a combination of both narrower and wider micropores (large S_{BET} and A_{CO2} values in Fig. 2C). Particularly, the volume of

ultramicropores (d < 0.7 nm) in the ec-biochar and nc-biochar were 0.226 and 0.169 cm^3/g, giving rise to specific surface areas ($A_{DR}(CO_2)$) of 625 and 395 m^2/g, respectively (Fig. 2C). Third, the concentration of oxygen surface groups in the biochar materials (between 2200-6600 µmol O/g) was remarkably larger compared to ec-coke (Fig. 2E). In this case, however, the largest amount of these functionalities corresponded to the nc-biochar. Besides, the figure distinguishes between both the CO_2- and CO-evolving groups. Deconvolution of TPD profiles (Fig. S3) [41] indicated that carboxylic-like functionalities stand out among the CO_2-evolving groups, while phenolic and carbonyl/quinone ones clearly prevail among the CO-evolving ones. The former could participate in the interaction with the bacteria proteins and/or biomolecules, whereas the last groups have been associated to electron transfer processes with electroactive bacteria [19].

To study the growth of biofilms in the different granules, their surface was explored by scanning electron microscope (SEM). As shown in Fig. S6, granules from the top and bottom layer of each system (planted and unplanted) were taken after 20 days of operation. At the top of the four planted beds, roots were clearly visible. These structures served as support for bacterial growth and had a positive effect on the microbial community, promoting greater morphological and species diversity. Furthermore, filamentous species, like phylum Actinobacteria, were very present on the surface of the granules of both biochar-based beds (Fig. S9). Furthermore, in the upper granules of the non-planted systems a high morphological diversity was observed, while no filamentous species were present in the gravel pebbles. This density and diversity of species can be attributed to the presence of aerophilic or microaerophilic species (Table S6 and S7). In the granules of the bottom layers, differences were only found between materials, and not due to the effect of the plant. The SEM micrographs of the gravel granules showed a biofilm that was visually less dense. As for the granules of carbonaceous materials, biofilms developed as a compact and

homogeneous layer of cells, which even penetrated through the channels presented in the biochar-based materials.

3.2 Performance of the bioelectrochemically-assisted treatment: what, how and who

The impact of the bed material was evaluated by measuring the COD and nitrogen removal efficiency in combination with the microbial biodiversity associated to the process. In addition, the growth of the plants was monitored to evaluate their role in the different bed materials. All biofilters were independently operated up-flow with urban real wastewater under continuous mode. Two stages were analysed separately: the start-up period (days 0-10) and the steady-state (days 10-20).

3.2.1 Removal of organic pollutants

The bioremediation of the organic pollutants present in urban wastewater was monitored through the evolution of COD values. Thus, some dependence between the electroconductivity of the material and bioremediation was observed from the very beginning of the assay during the start-up period (Fig. 3). Once steady-state was reached, METland® treatments led to removal rates as high as 175-180 gCOD/m^3day, outperforming gravel biofilter by 80 % (Table S2). Such material-mediated bioremediation generated effluents with COD values in a range as low as 70-80 mg/l, in contrast with effluents from gravel biofilter that were poorly cleaned-up (300-400 mg/l) under same HRT of two days (Fig. 3). In terms of performance, electroconductive bed (either ec-coke or ec-biochar) exhibited the best response, followed by the nc-biochar that still outperformed the gravel by 50-60 % (Table S1). If all that wastewater treatment (WWT) performance data are translated into the context of constructed wetlands (CW) we can anticipate our anaerobic electroconductive biofilters would accept a hydraulic loading rate as high as ca. 250 mm/day (0.6 m^2/pe) in contrast with the typical values of 30 mm/day (3-5 m^2/pe) used in constructed wetlands

operated under horizontal subsurface flow rate [42]. Indeed, such design values are in the same range of METland® units already constructed for treating urban wastewater [23].

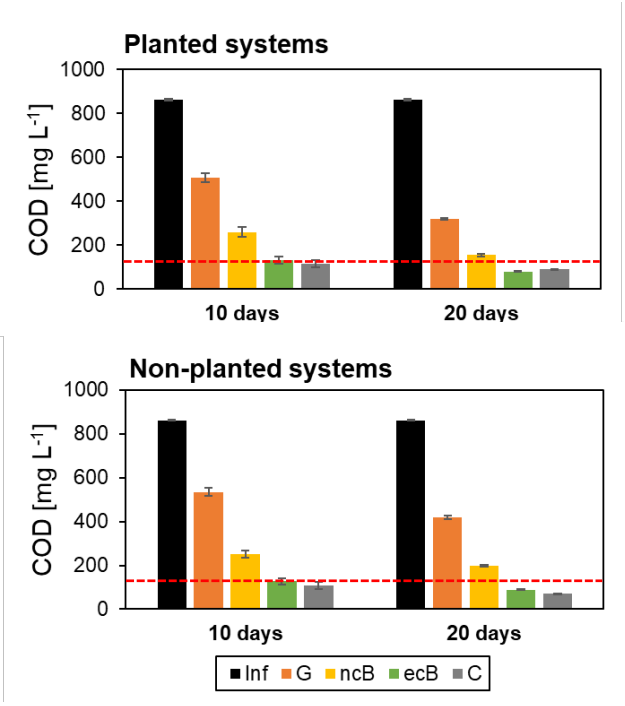

Fig. 3. COD concentration at the influent (black) and effluent of every biofilter: gravel (orange), nc-biochar (yellow), ec-biochar (green) and ec-coke (grey), operating up flow during 0-10 days and 10-20 days, in the planted systems (up) and non-planted systems (down). Red line: European discharge limit = 125 mg/L (Council Directive 2000/60/EC of 23 October 2000).

To gain further insight into the different performance of the different biofilters, we proceed to analyse the composition of the microbial communities colonizing all bed materials (Fig. 4). Once the biofilters were operated under steady-state regime, the gravel (control biofilter) was mainly colonized by bacteria from genus *Clostridium*. Such strictly anaerobic *Clostridium* populations were likely responsible for the rapid fermentation of carbohydrates from wastewater [43]. In contrast, in all our carbon-based biofilters systems, the most abundant genus was *Trichococcus,* an aerotolerant genus that was reported as electrode colonizer elsewhere [44,45]. Furthermore, species of this genus were described to perform direct or hydrochar-mediated EET inside anaerobic digesters [46,47]. *Trichococcus* typically exhibits a fermentative metabolism, capable to convert sugars and polysaccharides

into acetate. Interestingly, acetate is the main electron donor for bacteria from the genus *Geobacter*, the model microorganism in electromicrobiology [48,49], also detected by Illumina sequencing in our electroconductive biofilters but not in the inert gravel systems. Finally, it should be noted that *Pseudomonas* were detected in the upper locations of the systems, especially those made of biochar-based materials. Some species of this genus have been described as electroactive, such as *Pseudomonas aeruginosa*, *Pseudomonas alcaliphila* and *Pseudomonas fluorescens* (Table S7). In ours assays the most abundant species were *Pseudomonas xanthomarina* and *Pseudomonas guangdongensis,* also detected in an electroactive biofilm as organic acids oxidizer [50].

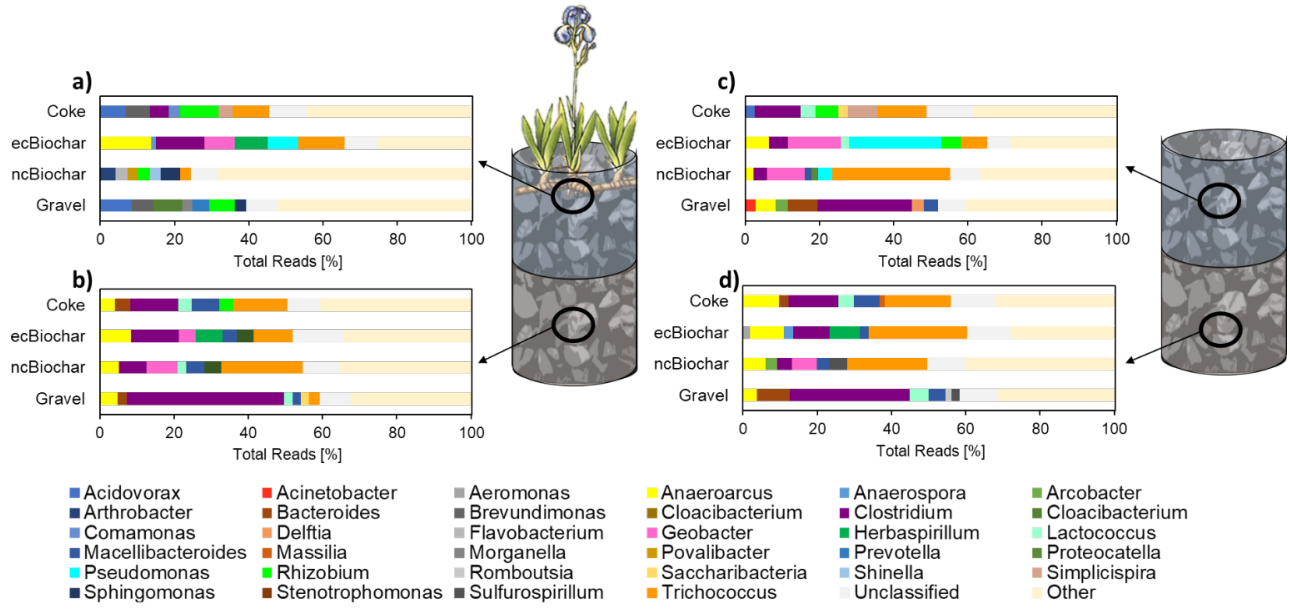

Fig. 4. The bar graph shows the relative abundance at genus-level. The figure shows the most important genera in each region of each system: a) upper layer of planted systems, b) lower layer of planted systems, c) upper layer of non-planted systems and d) lower layer of non-planted systems.

3.2.2 Removal of nitrogen

All systems were fed with urban wastewater free of either nitrate or nitrite but with a constant concentration of ammonium (65 mg/l). Ammonium removal was vastly affected by the bed material and, to a lesser extent, by the growth of plants from *Iris sibirica*. During the starting up period, all biochar-based biofilters already supported ammonium removal as high as 78

%, in contrast with gravel, that showed a very poor response if any at all (Table S3). However, once the system reached the steady state, all planted systems exhibited ammonium removal efficiency in a range from 40-80 % (Fig. 5). Furthermore, the presence of plants led to increase the efficiency exhibited by non-planted systems by 10-20 %. Interestingly, in terms of the material, ammonium removal was the highest in planted biochar-based biofilters (>80 %).

Ammonium removal from effluents can occur via microbial assimilation or nitrification. The last is a typically (but not exclusive) oxygen-based two-step process, where ammonium is first converted to nitrite by ammonia oxidizing bacteria (AOB) from Nitrosomonadales order. Then, the nitrite is converted into nitrate by nitrite-oxidizing bacteria (NOB) [40]. The high-throughput sequencing analysis for microbial biodiversity (Table S4) revealed that AOB reads were high enough in all systems to support the existence of ammonium oxidation. However, the number of AOB reads was slightly higher in gravel, what correlates with a greater impact of vegetation regarding ammonium removal. This could be related with the fact that plants adapted to flooded conditions present the ability to supply oxygen from the atmosphere to their roots providing a terminal electron acceptor (TEA) for nitrification. In absence of plants, such a TEA role could be played by carbonaceous material, like ec-coke, ec-biochar and nc-biochar biofilters in a similar way that annamox bacteria oxidize ammonium in absence of oxygen. Indeed, some anammox bacteria seem to couple NH_4^+ oxidation to the reduction of carbon-based insoluble extracellular electron acceptors [51,52]. In this context, Planctomycetes was an anammox bacteria detected in our carbon-based biofilters, representing in all cases a significant increase compared to the influent. Species of this order, such as those from genera *Brocadia, Kuenenia, Jettenia* and *Anammoxoglobus* are able to anaerobically oxidize ammonium, using NO_2^- or NO as intracellular electron acceptor [53,54]. METlands®, made of electroconductive coke or ec-biochar, could be good

environments for the development of such microbial populations. Actually, EET-dependent anammox process may outperform conventional anammox process by avoiding the production of greenhouse gas like N_2O. The actual role of such annamox communities in our ec-biochar for enhancing anaerobic ammonium removal is being currently investigated.

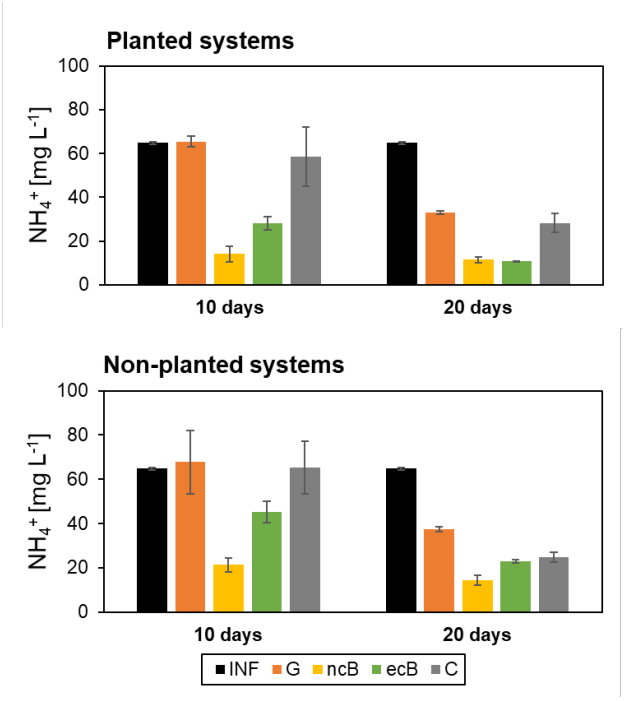

Fig. 5. NH_4^+ concentration at the influent (black) and effluent of every biofilter: gravel (orange), nc-biochar (yellow), ec-biochar (green) and ec-coke (grey), operating up flow during 0-10 days and 10-20 days, in the planted systems (up) and non-planted systems (down).

Denitrification is the second stage of the elimination of nitrogen in wastewater, which typically occurs under anoxic conditions by denitrifying bacteria (DNB). Interestingly, neither nitrate nor nitrite were detected in the effluent from our biofilters, suggesting that it was effectively consumed by DNB associated to the electroactive biofilm. The number of readings for these bacteria was always higher in biofilters made of carbon-based materials, at least twice as compared to the gravel system (Table S4). Dissimilatory nitrate reduction to ammonium (DNRA) is also possible in a two steps process via nitrite without intermediates [55]. The read numbers of DNRA bacteria were significantly higher in gravel systems and

ec-coke system, what could correlate well with the lower removal of total nitrogen in such systems.

3.2.3 Performance in planted and non-planted biofilters

Iris sibirica acclimatized and grew well in presence of wastewater with all different materials as substrate. Gas transport from the air sections of the plant into the rhizome fine roots is driven by specific areas of tissue known as aerenchyma. The release of oxygen in the roots causes the formation of an oxidative protective film directly on the root surface with a thickness between 1-4 mm [56,57]. This constant release of oxygen in the rhizosphere led to a great diversity at the very top of the biofilters, with the nitrogen fixing genera *Rhizobium* and *Herbaspirillum as* the most abundant (Fig. S10). Although the plant roots supplied oxygen, it was quickly consumed by the aerobic rhizosphere microorganisms, so oxygen was not detected along the depth of the systems and the water column was naturally kept under anoxic conditions. Thus, at the bottom location of every biofilter no major differences between the planted and non-planted systems were detected in terms of microbial biodiversity (Fig. 4 and table S5). This is consistent with the fact that rhizosphere did not reach the deep layers, so the differences in the microorganisms populations will be just a consequence of the effect of the bed material.

3.3 Electrochemical characterization of biofilter beds in lab-scale METlands®

3.3.1 Electric potentials depth profiles

It is well known that the up-flow operation of a conventional biofilter made of an inert material (gravel) typically leads to a microbial metabolism limited by the availability of a terminal electron acceptor [22]. Thus, in this system oxidation of pollutants and reduction of terminal electron acceptors are decoupled both temporally and spatially [22]. In contrast, our METland® design overcomes these limitations by means of an electrically conductive

material capable of transferring electrons from deeper layers, where the oxidation of organic pollutants mainly occurs (anodic reactions), towards the uppermost layers, where reduction reactions predominate (cathodic reactions). In this sense, a METland® under up-flow configuration operates as a single electrode (the so-called snorkel mode), so that, unlike standard microbial electrochemical systems [38], the absence of an external circuit impedes the electrical current to be directly measured. Instead, the flux of electrons through the biofilter beds was estimated by monitoring the electric potential profiles along the bed (Fig. 6) as it has been previously reported [6,22,58].

The relation between the in-depth EP profiles and the microbial activity and materials properties was first analyzed. The EP profile in the very early stage of operation (time 0) was negligible (the electrode potential was roughly zero), even for electroconductive systems (see the results “abiotic” in Figure 6). Initially, these materials did not have microorganisms grown on the surface. Without electroactive communities capable of oxidizing organic compounds and donate electrons to the material, hence, there was no flux of electrons (Fig. 6).

Over time, however, EP profiles became wider because of the electroactive biofilm development. Thus, once the steady state was reached (20 days), the microbial oxidation of organic pollutants was high enough to support a vertical flux of electrons towards the uppermost layers. Under these steady-state conditions, significant differences were observed among the EP profiles of the tested systems (Fig. 6), thus, reflecting the impact of the bed material on the flux of ions and, consequently, on the flux of electrons. Notably, the absence of an in-depth EP profile (Fig. 6) in the case of gravel may indicate that such an inert material cannot support electron flux along the bed. In a similar way, the flat in-depth EP profiles observed for the nc-biochar system (Fig. 6) may be due to the high ohmic resistance of this material. However, the lack of conductivity did not prevent it from playing

a role as geobattery, a mechanism based on the hydroquinonequinone (HQ/Q) reversible redox reaction able to stimulate microbial activity [19,31]. In contrast, biofilters made of electrically conductive materials, ec-biochar and ec-coke, showed a remarkable EP response with depth, confirming an electron transfer in the vertical axis (Fig. 6). The electrons produced by the EAB migrated to the uppermost material because of the redox gradient. The electrically conductive materials resistance also affected the EP profiles. The lower material resistance (ec-coke system, system with less ohmic drop), the greater flux of electrons. Interestingly, the biofilter made of ec-biochar showed a miscellaneous behavior: geoconductor and geobattery. An EP depth profile could be observed due to some electroconductivity of the material (geoconductor mechanism), but flatter than the ec-coke EP profile. Interestingly, as a consequence of the electrical resistance of the material, the bottom section showed an ohmic drop impact greater than the one from redox gradient, which makes geobattery processes predominate, promoting the presence of electroactive microorganisms (Table S4) with mediated electron transfer. Those electrons donated to carbon-bound mediators, such as quinones and humic-like material, will not migrate to the upper layers of the bed and, therefore, will not contribute to the EP profile slope.

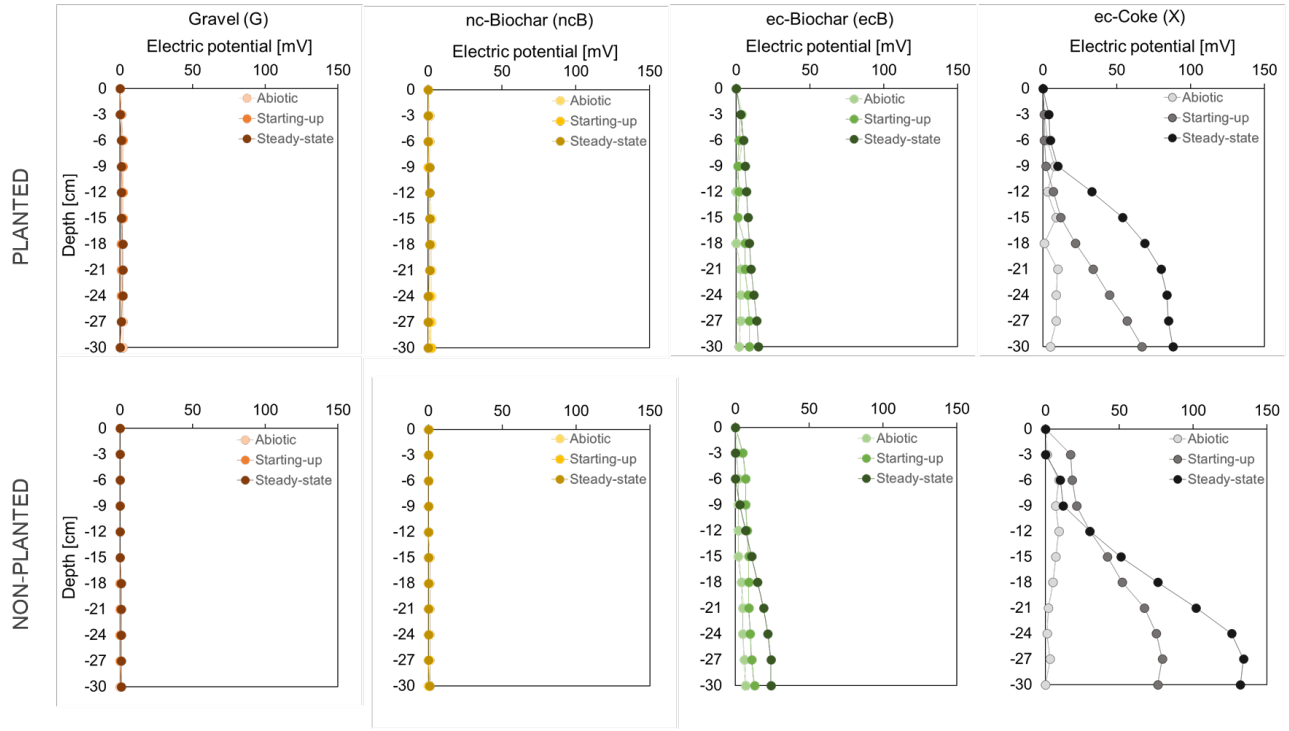

Fig. 6. Electric potential (EP) depth profiles of tested biofilters along depth at each time (abiotic, 10 days and 20 days) of gravel (orange), nc-biochar (yellow), ec-biochar (green) and ec-coke (grey) bed, in planted (up) and non-planted (down) systems. EP profiles were measured with a shielded Ag/AgCl electric potential electrode.

The use of vegetation (Fig. 6 up) should generate a greater vertical redox gradient since the roots were supplying oxygen into the system. However, we did not observe such an effect. A possible reason may be that this oxygen would be directly consumed by rhizosphere-associated communities in presence of organic compounds from root exudates [59,60]. If so, oxygen would not be really available for cathodophilic bacteria associated to the uppermost layer of the electroconductive material. This was confirmed by the highest concentration of bacteria of the genus *Rhizobium* found in the upper layer of the planted systems (Fig. S9).

3.3.2 Cyclic voltammetry of single granules

Cyclic voltammetry (CV) is a standard electrochemical tool to characterize electron transfer between microorganisms or biofilms and electrodes [61,62], through direct detection of redox signals and electrochemical reactions [7]. To investigate the evolution of the biofilm

and determine the electrochemical activity of the electrode materials, single granules CVs were performed at different stages of biofilm formation (day 0, starting-up and steady-state) from different bed locations (upper and bottom layer). CVs were recorded during non-turnover (NTO), conditions in absence of electron donor. Application of certain potentials can disrupt biofilms either by producing hydrogen [63] or by inducing unfolding/ oxidation of adsorbed proteins at oxidizing potentials [64], so we just performed the analyses at a scan rate of 10 mV/s from 0.6 V to -0.6V vs. Ag/AgCl.

Independent granules were taken from the system just before the electrochemical analysis, and their electrical resistivity was measured. A first round of CV was performed on granules from ec-coke (2 Ω/cm), ec-biochar (20 Ω/cm) and nc-biochar (200 Ω/cm) at time 0 to identify redox signals in biofilm-free material. The slope of the voltammogram was directly proportional to the ohmic resistance of the material (Fig. S7, S8 and S9). Despite the resistance of the materials, no redox peaks were observed before microbial colonization.

In the case of nc-biochar no redox peaks were observed in material at the start-up and steady-state stages. This is consistent with the poor conductive nature of the material. However, after 20 days of operation (steady-state) the slope of the voltammograms increased with time, as well as the capacitive current recorded in all the granules (Fig. S7). This could be explained, because the biofilm growth may have clogged the micro and mesopores, reducing the flow of ions and, therefore, increasing the resistance due to ohmic drop.

In the case of ec-biochar granules (Fig. S8), an evolution of the voltammograms was observed over time. During the start-up process, an increase in capacity was observed. Furthermore, the capacitive current of the voltammograms after 20 days together with the electric resistance of the material, might mask the presence of small faradaic currents from

microbial nature. Slow reactions may not be detected because due to the fast potential shifts caused by the scan rate. Thus, as the scan rate increases, the kinetics of interfacial electron transfer between redox proteins and electrodes strongly affects the voltametric response, even hiding the kinetics of continuous enzymatic turnover. The fact that no clear CV shape was observed for ec-biochar granules could also suggest that such material was originally colonized by mediator-based electroactive community and, unfortunately soluble redox mediator cannot be detected when a single granule was analysed in an independent electrochemical cell.

Finally, the CVs curves of the ec-coke systems under non-turnover condition (Fig. 7) revealed that formal potentials from all voltammograms were similar and in accordance with literature data typical for wastewater-derived biofilm and the oxidation and reduction peaks evidenced the presence of redox-active species [65,66]. In contrast with the biochar-based analysis, the CVs of the ec-coke granules (Fig. S9) showed the greatest evolution over time. From a very flat voltammogram in biofilm-free granules, the material evolved to eventually show a capacitive current and slight oxidation after 10 days of operation. Once steady-state was reached, such features became more remarkable and the capacitive current was considerably higher than the bioelectrocatalytic current densities. This capacitive current was due to a non-catalytic activity, because the presence of both redox-active microbiological moiety and exo-polysaccharide matrix. To calculate the formal potential of the oxidation-reduction pair that appeared in the upper planted and lower non-planted ec-coke systems the first derivative of such CVs (steady-state) was performed (Fig. S10). The formal potential value for the redox pairs that appeared, E_0 = -220 mV (vs. the Ag / AgCl), was in accordance with the literature data for non-turnover CVs of biofilms enriched from primary wastewater [67,68]. On the other hand, the voltagram recorded on the granule of the non-planted bottom ec-coke system (Fig. 7) showed a redox couple. The formal potential

was -201 mV (vs. the Ag / AgCl). Similar responses have been previously reported for the oxidation of acetate by biofilms of single culture *Geobacter sulfurreducens* [69,70]. The currents densities reached under steady-state were probably the result of a higher cell density at the electrode surface or higher expression of membrane-bound electron transfer proteins [62]. This is confirmed by the presence of to the microbial community results (Table. S4) since in the ec-coke systems, electroactive community with direct electron transfer were more abundant than the mediated electron transfer, while the second was the most common in biochar materials.

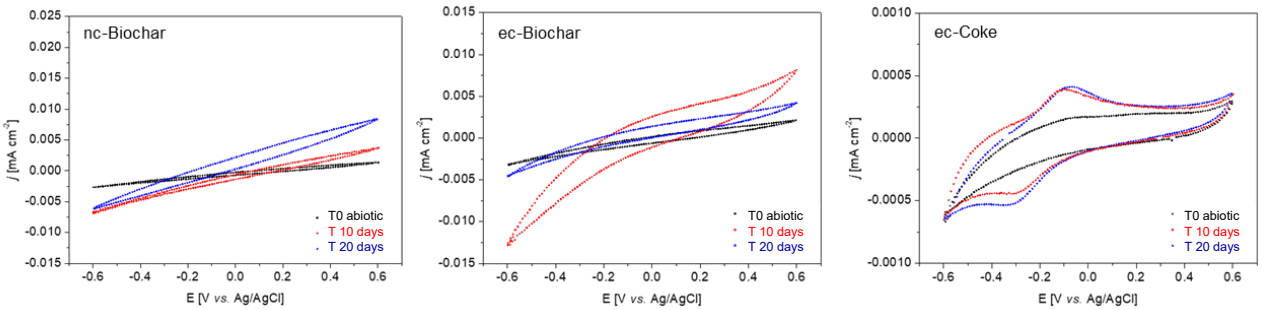

Fig. 7. Cyclic voltammograms of a single granule of nc-biochar, ec-biochar and ec-coke from the non-planted bottom system at different stages (biofilm-free (black), 10 days (red) and 20 days (blue)). Scan rate 10 mV/s; phosphate buffer 100mM, acetate 10mM.

3.4 Geobacter as key actor in electrochemical syntrophies

Microbial extracellular electron transfer, either in form of DIET (Direct Interspecies Electron Transfer) or CIET (Conductive-particle-mediated Interspecies Electron Transfer) is currently "trending topic" in environmental biotechnology field [71]. Thus, such kind of syntrophies have a key role in engineering applications for treating brewery wastewater in anaerobic digestors [72] or microbial electrochemical fluidized bed reactors [73,74]. In this context, the nature of the material determines how extracellular electron transfer can be stimulated. In our case, electrically conductive minerals, such as ec-coke, promote the transfer of electrons through electronic channels and depends on the electrically conductivity of the material. In

biochar materials, humic-like substances are also present acting as electron acceptors for microbial respiration [75–77].

In such syntrophic interactions, electroactive microorganism like those from genus *Geobacter* play a key role [29,78]. So, we evaluated its relative abundance in our biofilters, both at genus and species level (Fig. 8).

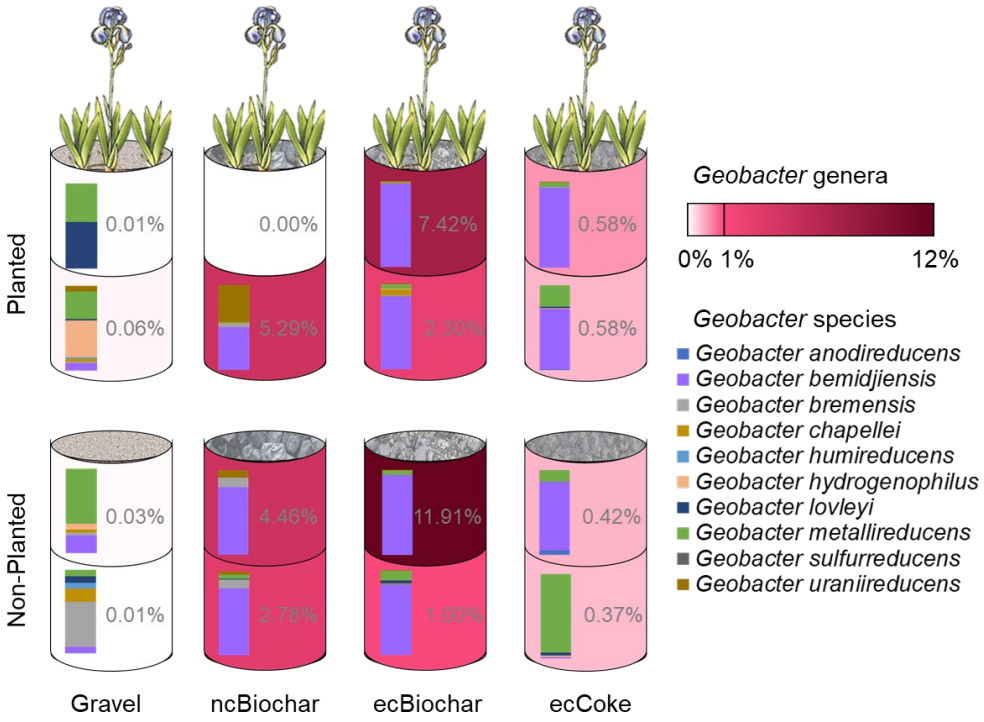

Fig. 8. Relative abundance of *Geobacter* (represented with pink colour intensity) at different locations from biofilters made of a) gravel, b) nc-biochar, c) ec-biochar and d) ec-coke. In bar graph: percentage of each *Geobacter* species of the total registered for each location.

The highest presence of *Geobacter* occurred in the carbonaceous materials, especially in the electrically conductive biochar (12 %); probably due to the presence of quinone-like groups on the surface [79]. In the carbonaceous materials, *Geobacter bemidjiensis* seem to predominate among all *Geobacter* genus detected. Interestingly, this specie can couple not just acetate oxidation but also end-products (butanol, ethanol, formate, lactate) from fermenters to the reduction of EET respiration [80,81]. In contrast, the percentage of *Geobacter* found in the gravel bed was no more than 0.05 %, with no clear dominance of a

specific species. To conclude, the high presence of *Geobacter* species can be related to the higher COD removal efficiency and, in turn, i) to those electrical potential profiles showing slope and ii) to the cyclic voltammetry with higher peaks for oxidation peaks and reduction. This occurs in the ec-Biochar biofilter, a bed material that has proven to be the best for the most efficient treatment of wastewater.

4. Conclusions

In conclusion, the use of electroconductive carbon-based materials for the construction of biofilters like METland® are capable of stimulating electroactive microbial communities to perform an efficient extracellular electron transfer and, eventually, greatly enhance pollutants removal in wastewater. The low resistance of materials like electroconductive coke allow to operate METland® following a pure geoconductor mechanism. However, the fact that sustainable materials like biochar exhibit phenolic and carbonyl/quinone groups able to support electron transfer opens an interesting field for exploring new concepts in wastewater treatment. Indeed, the existence of such a geobattery mechanism suggests that electroconductivity of the material is not necessarily the only feature for selecting a material to grow electroactive microbial communities like *Geobacter*. Ideally, we should deeply investigate those materials able to couple, even spatially distant, microbial redox reactions and accordingly carry out specific syntrophic and/or cooperative metabolisms to maximize pollutant biodegradation.

Declaration of Competing Interest

The authors declare that they have no known competing financial interests or personal relationships that could have appeared to influence the work reported in this paper.

Acknowledgement

The authors thank the MINECO and FEDER (RYC-2017-23618) for financial support. This investigation has received funding from the European Union's Horizon 2020 research and innovation programme under the grant agreements No. 826244 (Project “ELECTRA”; http://www.electra.site). Amanda Prado de Nicolás was funded by the “Formación de Personal Investigador (FPI)” PhD fellowship programme from the University of Alcalá.

Appendix A. Supplementary data

The following are the Supplementary data to this article.

5. References

[1] N. Faivre, M. Fritz, T. Freitas, B. de Boissezon, S. Vandewoestijne, Nature-Based Solutions in the EU: Innovating with nature to address social, economic and environmental challenges, Environ. Res. 159 (2017) 509–518. doi:10.1016/j.envres.2017.08.032.

[2] H. Brix, Constructed wetlands for municipal wastewater treatment in Europe. In: Mitsch, W.J. (Ed.), Global Wetlands: Old World and New, (1994) 325–334. doi:ISBN 13: 9780444814784.

[3] H. Brix, Plants used in constructed wetlands and their function, Semin. Use Aquat. Macrophytes WWT CW. (2003) 2–30.

[4] J. Vymazal, The use constructed wetlands with horizontal sub-surface flow for various types of wastewater, 5 (2008) 1–17. doi:10.1016/j.ecoleng.2008.08.016.

[5] R. Kadlec, S. Wallace, Ttreatment wetlands, in: Vasa, 2009: p. 1048. ISBN 13: 9781566705264.

[6] C.A. Ramírez-Vargas, C.A. Arias, P. Carvalho, L. Zhang, A. Esteve-Núñez, H. Brix, Electroactive biofilm-based constructed wetland (EABB-CW): A mesocosm-scale test of an innovative setup for wastewater treatment, Sci. Total Environ. 659 (2019) 796–806. doi:10.1016/j.scitotenv.2018.12.432.

[7] A. Esteve-Núñez, J.P. Busalmen, A. Berná, C. Gutiérrez-Garrán, J.M. Feliu, Opportunities behind the unusual ability of geobacter sulfurreducens for exocellular respiration and electricity production, Energy Environ. Sci. 4 (2011) 2066–2069. doi:10.1039/c1ee01067k.

[8] X. Wang, F. Aulenta, S. Puig, A. Esteve-Núñez, Y. He, Y. Mu, K. Rabaey, Microbial electrochemistry for bioremediation, Environ. Sci. Ecotechnology. 1 (2020) 100013. doi:10.1016/j.ese.2020.100013.

[9] C.A. Ramírez-Vargas, A. Prado, C.A. Arias, P.N. Carvalho, A. Esteve-Núñez, H. Brix, Microbial electrochemical technologies for wastewater treatment: Principles and evolution from microbial fuel cells to bioelectrochemical-based constructed wetlands, Water (Switzerland). 10 (2018). doi:10.3390/w10091128.

[10] L. Doherty, Y. Zhao, X. Zhao, W. Wang, Nutrient and organics removal from swine slurry with simultaneous electricity generation in an alum sludge-based constructed wetland incorporating microbial fuel cell technology, Chem. Eng. J. 266 (2015) 74–81. doi:10.1016/j.cej.2014.12.063.

[11] F. Xu, F. qian Cao, Q. Kong, L. lu Zhou, Q. Yuan, Y. jie Zhu, Q. Wang, Y. da Du, Z. de Wang, Electricity production and evolution of microbial community in the constructed wetland-microbial fuel cell, Chem. Eng. J. 339 (2018) 479–486. doi:10.1016/j.cej.2018.02.003.

[12] C. Corbella, M. Guivernau, M. Viñas, J. Puigagut, Operational, design and microbial aspects related to power production with microbial fuel cells implemented in constructed wetlands, Water Res. 84 (2015) 232–242. doi:10.1016/j.watres.2015.06.005.

[13] A.K. Yadav, P. Dash, A. Mohanty, R. Abbassi, B.K. Mishra, Performance assessment of innovative constructed wetland-microbial fuel cell for electricity production and dye removal, Ecol. Eng. 47 (2012) 126–131. doi:10.1016/j.ecoleng.2012.06.029.

[14] P. Srivastava, R. Abbassi, A. Yadav, V. Garaniya, M. Asadnia, T. Lewis, S.J. Khan, Influence of applied potential on treatment performance and clogging behaviour of hybrid

constructed wetland-microbial electrochemical technologies, Chemosphere. 284 (2021) 131296. doi:10.1016/j.chemosphere.2021.131296.

[15] L. Doherty, Y. Zhao, X. Zhao, Y. Hu, X. Hao, L. Xu, R. Liu, A review of a recently emerged technology: Constructed wetland – microbial fuel cells, Water Res. (2015). doi:10.1016/j.watres.2015.08.016.

[16] C. Corbella, J. Puigagut, Microbial fuel cells implemented in constructed wetlands: Fundamentals, current research and future perspectives, Contrib. to Sci. 11 (2015) 113–120. doi:10.2436/20.7010.01.220.

[17] C. Tang, Y. Zhao, C. Kang, Y. Yang, D. Morgan, L. Xu, Towards concurrent pollutants removal and high energy harvesting in a pilot-scale CW-MFC: Insight into the cathode conditions and electrodes connection, Chem. Eng. J. 373 (2019) 150–160. doi:10.1016/j.cej.2019.05.035.

[18] A. Aguirre-Sierra, T. Bacchetti-De Gregoris, A. Berná, J.J. Salas, C. Aragón, A. Esteve-Núñez, Microbial electrochemical systems outperform fixed-bed biofilters in cleaning up urban wastewater, Environ. Sci. Water Res. Technol. 2 (2016) 984–993. doi:10.1039/c6ew00172f.

[19] A. Prado, R. Berenguer, A. Esteve-Núñez, Electroactive biochar outperforms highly conductive carbon materials for biodegrading pollutants by enhancing microbial extracellular electron transfer, Carbon N. Y. 146 (2019). doi:10.1016/j.carbon.2019.02.038.

[20] Á. Pun, K. Boltes, P. Letón, A. Esteve-nuñez, Bioresource Technology Reports Detoxification of wastewater containing pharmaceuticals using horizontal flow bioelectrochemical filter, Bioresour. Technol. Reports. 7 (2019) 100296. doi:10.1016/j.biteb.2019.100296.

[21] B. Erable, L. Etcheverry, A. Bergel, From microbial fuel cell (MFC) to microbial electrochemical snorkel (MES): maximizing chemical oxygen demand (COD) removal from wastewater, Biofouling. 27 (2011) 319–326. doi:10.1080/08927014.2011.564615.

[22] A. Prado, C.A. Ramírez-Vargas, C.A. Arias, A. Esteve-Núñez, Novel bioelectrochemical strategies for domesticating the electron flow in constructed wetlands, Sci. Total Environ. 735 (2020) 139522. doi:10.1016/j.scitotenv.2020.139522.

[23] iMETland European H2020 project., http://imetland.eu/.

[24] L. Peñacoba-Antona, J. Senán-Salinas, A. Aguirre-Sierra, P. Letón, J.J. Salas, E. García-Calvo, A. Esteve-Núñez, Assessing METland® design and performance through LCA: techno-environmental study with multifunctional unit perspective., Front. Microbiol. 12 (2021) 1331. doi: 10.3389/fmicb.2021.652173

[25] C.C. Tanner, Plants for constructed wetland treatment systems — A comparison of the growth and nutrient uptake of eight emergent species, Ecol. Eng. 7 (1996) 59–83. doi:10.1016/0925-8574(95)00066-6.

[26] T. Koottatep, C. Polprasert, Role of plant uptake on nitrogen removal in constructed wetlands located in the tropics, Water Sci. Technol. 36 (1997) 1 LP – 8. http://wst.iwaponline.com/content/36/12/1.abstract.

[27] L. Zhang, T. Lyu, C.A. Ramírez Vargas, C.A. Arias, P.N. Carvalho, H. Brix, New insights into the effects of support matrix on the removal of organic micro-pollutants and the microbial community in constructed wetlands, Environ. Pollut. 240 (2018) 699–708. doi:10.1016/j.envpol.2018.05.028.

[28] A. Aguirre-Sierra, Integrating microbial electrochemical systems in constructed wetlands, a new paradigm for treating wastewater in small communities, Universidad de Alcalá, Spain, 2017.

[29] A.E. Rotaru, M.O. Yee, F. Musat, Microbes trading electricity in consortia of environmental and biotechnological significance, Curr. Opin. Biotechnol. 67 (2021) 119–129. doi:10.1016/j.copbio.2021.01.014.

[30] S. Tejedor-Sanz, P. Fernández-Labrador, S. Hart, C.I. Torres, A. Esteve-Núñez, Geobacter

Dominates the Inner Layers of a Stratified Biofilm on a Fluidized Anode During Brewery Wastewater Treatment , Front. Microbiol. 9 (2018) 378. doi: 10.3389/fmicb.2018.00378.

[31] T. Sun, B.D.A. Levin, J.J.L. Guzman, A. Enders, D.A. Muller, L.T. Angenent, J. Lehmann, Rapid electron transfer by the carbon matrix in natural pyrogenic carbon, Nat. Commun. 8 (2017) 1–12. doi:10.1038/ncomms14873.

[32] T. Sun, J.J.L. Guzman, J.D. Seward, A. Enders, J.B. Yavitt, J. Lehmann, L.T. Angenent, Suppressing peatland methane production by electron snorkeling through pyrogenic carbon in controlled laboratory incubations, Nat. Commun. 12 (2021) 4119. doi:10.1038/s41467-021-24350-y.

[33] I. Miccoli, F. Edler, H. Pfnür, C. Tegenkamp, The 100th anniversary of the four-point probe technique: the role of probe geometries in isotropic and anisotropic systems, J. Phys. Condens. Matter. 27 (2015) 223201. doi: 10.1088/0953-8984/27/22/223201

[34] F. Béguin, E. Frackowiak, Carbons for electrochemical energy storage and conversion systems, Crc Press, 2009. ISBN: 9780429141256.

[35] S. Lowell, J.E. Shields, M.A. Thomas, M. Thommes, Characterization of porous solids and powders: surface area, pore size and density, Springer Science & Business Media, 2012. ISBN: 1-4020-2302-2.

[36] J.L. Figueiredo, M.F.R. Pereira, M.M.A. Freitas, J.J.M. Orfao, Modification of the surface chemistry of activated carbons, Carbon N. Y. 37 (1999) 1379–1389. doi: 10.1016/S0008-6223(98)00333-9

[37] APHA/AWWA/WEF, Standard Methods for the Examination of Water and Wastewater, 2012. doi:ISBN 9780875532356.

[38] A. Prado, R. Berenguer, A. Berná, A. Esteve-Núñez, Simultaneous characterization of porous and non-porous electrodes in microbial electrochemical systems, MethodsX. 7 (2020). doi:10.1016/j.mex.2020.101021.

[39] A. Klindworth, E. Pruesse, T. Schweer, J. Peplies, C. Quast, M. Horn, F.O. Glöckner, Evaluation of general 16S ribosomal RNA gene PCR primers for classical and next-generation sequencing-based diversity studies, Nucleic Acids Res. 41 (2013) 1–11. doi:10.1093/nar/gks808.

[40] A. Aguirre-Sierra, T. Bacchetti-De Gregoris, J.J. Salas, A. De Deus, A. Esteve-Núñez, A new concept in constructed wetlands: Assessment of aerobic electroconductive biofilters, Environ. Sci. Water Res. Technol. 6 (2020) 1312–1323. doi:10.1039/c9ew00696f.

[41] L.J. Lemus-Yegres, I. Such-Basáñez, M.C. Román-Martínez, C.S.-M. De Lecea, Catalytic properties of a Rh–diamine complex anchored on activated carbon: effect of different surface oxygen groups, Appl. Catal. A Gen. 331 (2007) 26–33. doi:10.1016/j.apcata.2007.07.020

[42] J. García, J. Vivar, M. Aromir, R. Mujeriego, Role of hydraulic retention time and granular medium in microbial removal in tertiary treatment reed beds, Water Res. 37 (2003) 2645–2653. doi:10.1016/S0043-1354(03)00066-6.

[43] P. Dürre, Physiology and sporulation in Clostridium, Bact. Spore from Mol. to Syst. (2016) 313–329. doi:10.1128/microbiolspec.TBS-0010-2012

[44] G. Zhao, F. Ma, L. Wei, H. Chua, C. Chang, X. Zhang, Electricity generation from cattle dung using microbial fuel cell technology during anaerobic acidogenesis and the development of microbial populations, Waste Manag. 32 (2012) 1651–1658. doi:10.1016/j.wasman.2012.04.013.

[45] S. Saheb-alam, F. Persson, Response to starvation and microbial community composition in microbial fuel cells enriched on different electron donors, (2019). doi:10.1111/1751-7915.13449.

[46] G. Baek, J. Kim, K. Cho, H. Bae, C. Lee, The biostimulation of anaerobic digestion with (semi)conductive ferric oxides: their potential for enhanced biomethanation, Appl. Microbiol. Biotechnol. 99 (2015) 10355–10366. doi:10.1007/s00253-015-6900-y.

[47] S. Ren, M. Usman, D.C.W. Tsang, O. Sompong, I. Angelidaki, X. Zhu, S. Zhang, G. Luo, Energy and Climate Hydrochar-facilitated anaerobic digestion : Evidence for direct interspecies electron transfer mediated through surface oxygen-containing functional groups, (2020). doi:10.1021/acs.est.0c00112.

[48] J.P. Busalmen, A. Esteve-Núñez, C - Type Cytochromes Wire Electricity - Producing Bacteria to Electrodes C-Type Cytochromes Wire Electricity-Producing Bacteria to Electrodes **, (2017) 4952–4955. doi:10.1002/ange.200801310.

[49] D.R. Lovley, D.J.F. Walker, Geobacter Protein Nanowires , Front. Microbiol. . 10 (2019) 2078. doi:10.3389/fmicb.2019.02078.

[50] G. Yang, L. Han, J. Wen, S. Zhou, Pseudomonas guangdongensis sp. nov., isolated from an electroactive biofilm, and emended description of the genus Pseudomonas Migula 1894, Int. J. Syst. Evol. Microbiol. 63 (2013) 4599–4605. doi:10.1099/ijs.0.054676-0.

[51] D.R. Shaw, M. Ali, K.P. Katuri, J.A. Gralnick, J. Reimann, R. Mesman, L. van Niftrik, M.S.M. Jetten, P.E. Saikaly, Extracellular electron transfer-dependent anaerobic oxidation of ammonium by anammox bacteria, Nat. Commun. 11 (2020) 1–12. doi:10.1038/s41467-020-16016-y.

[52] A. Vilajeliu-Pons, C. Koch, M.D. Balaguer, J. Colprim, F. Harnisch, S. Puig, Microbial electricity driven anoxic ammonium removal, Water Res. 130 (2018) 168–175. doi:10.1016/j.watres.2017.11.059

[53] B. Kartal, W.J. Maalcke, N.M. De Almeida, I. Cirpus, J. Gloerich, W. Geerts, H.J.M. Op Den Camp, H.R. Harhangi, E.M. Janssen-Megens, K.J. Francoijs, H.G. Stunnenberg, J.T. Keltjens, M.S.M. Jetten, M. Strous, Molecular mechanism of anaerobic ammonium oxidation, Nature. 479 (2011) 127–130. doi:10.1038/nature10453.

[54] Z. Hu, H.J.C.T. Wessels, T. van Alen, M.S.M. Jetten, B. Kartal, Nitric oxide-dependent anaerobic ammonium oxidation, Nat. Commun. 10 (2019). doi:10.1038/s41467-019-09268-w.

[55] A. Pandey, H. Suter, J.Z. He, H.W. Hu, D. Chen, Dissimilatory nitrate ammonification and N2 fixation helps maintain nitrogen nutrition in resource-limited rice paddies, Biol. Fertil. Soils. 57 (2021) 107–115. doi:10.1007/s00374-020-01508-2.

[56] W. Armstrong, R. Brandle, J. M.B., Mechanism of Flood Tolerance Plants, Acta Bot. Neerl. 43 (1994) 307–358.

[57] B.B. Vartapetian, M.B. Jackson, Plant adaptations to anaerobic stress, Ann. Bot. 79 (1997) 3–20. doi:10.1006/anbo.1996.0295.

[58] L.R. Damgaard, N. Risgaard-Petersen, L.P. Nielsen, Electric potential microelectrode for studies of electrobiogeophysics, J. Geophys. Res. Biogeosciences. 119 (2014) 1906–1917. doi:10.1002/2014JG002665.

[59] V. V. Scholz, H. Müller, K. Koren, L.P. Nielsen, R.U. Meckenstock, The rhizosphere of aquatic plants is a habitat for cable bacteria, FEMS Microbiol. Ecol. 95 (2019). doi:10.1093/femsec/fiz062.

[60] V. V. Scholz, R.U. Meckenstock, L.P. Nielsen, N. Risgaard-Petersen, Cable bacteria reduce methane emissions from rice-vegetated soils, Nat. Commun. 11 (2020) 1–5. doi:10.1038/s41467-020-15812-w.

[61] J. Rodrigo Quejigo, L.F.M. Rosa, F. Harnisch, Electrochemical characterization of bed electrodes using voltammetry of single granules, Electrochem. Commun. 90 (2018) 78–82. doi:10.1016/j.elecom.2018.04.009.

[62] K. Fricke, F. Harnisch, U. Schro, On the use of cyclic voltammetry for the study of anodic electron transfer in microbial fuel cells, (2008) 144–147. doi:10.1039/b802363h.

[63] M.S. Gião, M.I. Montenegro, M.J. Vieira, The influence of hydrogen bubble formation on the removal of Pseudomonas fluorescens biofilms from platinum electrode surfaces, Process Biochem. 40 (2005) 1815–1821. doi:10.1016/j.procbio.2004.06.068.

[64] R.E. Perez-Roa, D.T. Tompkins, M. Paulose, C.A. Grimes, M.A. Anderson, D.R. Noguera,

Effects of localised, low-voltage pulsed electric fields on the development and inhibition of Pseudomonas aeruginosa biofilms, Biofouling. 22 (2006) 383–390. doi:10.1080/08927010601053541.

[65] K.P. Katuri, A.M. Enright, V. O'Flaherty, D. Leech, Microbial analysis of anodic biofilm in a microbial fuel cell using slaughterhouse wastewater, Bioelectrochemistry. 87 (2012) 164–171. doi:10.1016/j.bioelechem.2011.12.002.

[66] L. Zhuang, Y. Zheng, S. Zhou, Y. Yuan, H. Yuan, Y. Chen, Scalable microbial fuel cell (MFC) stack for continuous real wastewater treatment., Bioresour. Technol. 106 (2012) 82–8. doi:10.1016/j.biortech.2011.11.019.

[67] M. Pierra, A.A. Carmona-Martínez, E. Trably, J.J. Godon, N. Bernet, Microbial characterization of anode-respiring bacteria within biofilms developed from cultures previously enriched in dissimilatory metal-reducing bacteria, Bioresour. Technol. 195 (2015) 283–287. doi:10.1016/j.biortech.2015.07.010.

[68] A.A. Carmona-Martínez, F. Harnisch, U. Kuhlicke, T.R. Neu, U. Schröder, Electron transfer and biofilm formation of Shewanella putrefaciens as function of anode potential, Bioelectrochemistry. 93 (2013) 23–29. doi:10.1016/j.bioelechem.2012.05.002.

[69] C.I. Torres, R. Krajmalnik-Brown, P. Parameswaran, A.K. Marcus, G. Wanger, Y.A. Gorby, B.E. Rittmann, Selecting anode-respiring bacteria based on anode potential: Phylogenetic, electrochemical, and microscopic characterization, Environ. Sci. Technol. 43 (2009) 9519–9524. doi:10.1021/es902165y.

[70] E. Marsili, J.B. Rollefson, D.B. Baron, R.M. Hozalski, D.R. Bond, Microbial biofilm voltammetry: Direct electrochemical characterization of catalytic electrode-attached biofilms, Appl. Environ. Microbiol. 74 (2008) 7329–7337. doi:10.1128/AEM.00177-08.

[71] L. Shi, H. Dong, G. Reguera, H. Beyenal, A. Lu, J. Liu, H.Q. Yu, J.K. Fredrickson, Extracellular electron transfer mechanisms between microorganisms and minerals, Nat. Rev. Microbiol. 14 (2016) 651–662. doi:10.1038/nrmicro.2016.93.

[72] M. Morita, N.S. Malvankar, A.E. Franks, Z.M. Summers, L. Giloteaux, A.E. Rotaru, C. Rotaru, D.R. Lovley, Potential for Direct Interspecies Electron Transfer in Methanogenic Wastewater Digester Aggregates, MBio. 2 (2011) e00159-11. doi:10.1128/mBio.00159-11.

[73] S. Tejedor-Sanz, J.R. Quejigo, A. Berná, A. Esteve-Núñez, The Planktonic Relationship Between Fluid-Like Electrodes and Bacteria: Wiring in Motion, ChemSusChem. 10 (2017) 693–700. doi:10.1002/cssc.201601329.

[74] S. Tejedor-Sanz, P. Fernández-Labrador, C. Manchón, A. Esteve-Núñez, Fluidized bed cathodes as suitable electron donors for bacteria to remove nitrogen and produce biohydrogen, Electrochem. Commun. 116 (2020) 106759. doi:10.1016/j.elecom.2020.106759.

[75] S. Chen, A.E. Rotaru, P.M. Shrestha, N.S. Malvankar, F. Liu, W. Fan, K.P. Nevin, D.R. Lovley, Promoting interspecies electron transfer with biochar, Sci. Rep. 4 (2014). doi:10.1038/srep05019.

[76] D.R. Lovley, J.D. Coates, E.L. Blunt-Harris, E.J.P. Phillips, J.C. Woodward, Humic substances as electron acceptors for microbial respiration, Nature. 382 (1996) 445–448. doi:10.1038/382445a0.

[77] D.R. Lovley, J.L. Fraga, E.L. Blunt-Harris, L.A. Hayes, E.J.P. Phillips, J.D. Coates, D.R. Lovley, J.L. Fraga, E.L. Blunt-Harris, L.A. Hayes, E.J.P. Phillips, J.D. Coates, Humic Substances as a Mediator for Microbially Catalyzed Metal Reduction Huminstoffe als Vermittler bei der mikrobiell katalysierten Metallreduktion, Acta Hydrochim. Hydrobiol. 26 (1998).

[78] P.M. Shrestha, A.E. Rotaru, Plugging in or going wireless: Strategies for interspecies electron transfer, Front. Microbiol. 5 (2014) 1–9. doi:10.3389/fmicb.2014.00237.

[79] D.R. Lovley, Bug juice: harvesting electricity with microorganisms, Nat. Rev. Microbiol. 4 (2006) 497–508. doi:10.1038/nrmicro1442.

[80] K.P. Nevin, D.E. Holmes, T.L. Woodard, E.S. Hinlein, D.W. Ostendorf, D.R. Lovley, Geobacter bemidjiensis sp. nov. and Geobacter psychrophilus sp. nov., two novel Fe(III)-reducing subsurface isolates, Int. J. Syst. Evol. Microbiol. 55 (2005) 1667–1674. doi:10.1099/ijs.0.63417-0.

[81] C. Koch, F. Harnisch, Is there a Specific Ecological Niche for Electroactive Microorganisms?, ChemElectroChem. 3 (2016) 1282–1295. doi:10.1002/celc.201600079.